

Photoinduced proton transfer in 3-hydroxy-2-naphthoic acid

Hirdyesh Mishra^a, Hem Chandra Joshi^{a,1}, Hira Ballabh Tripathi^a, Shruti Maheshwary^b,
Narayanasami Sathyamurthy^{b,*,2}, Manoranjan Panda^c, Jayaraman Chandrasekhar^c

^a *Photophysics Laboratory, Department of Physics, Kumaun University, Nainital 263001, India*

^b *Department of Chemistry, Indian Institute of Technology, Kanpur 208016, India*

^c *Department of Organic Chemistry, Indian Institute of Science, Bangalore 560012, India*

Received 26 April 2000; received in revised form 18 October 2000; accepted 15 November 2000

Abstract

Spectral and photophysical properties of 3-hydroxy-2-naphthoic acid (3HNA) have been investigated experimentally and theoretically. In addition to its normal fluorescence, 3HNA exhibits a large Stokes-shifted emission that depends on its concentration, the nature of the solvent, pH, temperature and excitation wavelength. 3HNA seems to form different emitting species in different media. The large Stokes shift is attributed to species undergoing excited state intramolecular proton transfer (ESIPT). Ab initio calculations using configuration interaction (single excitation) reveal a single minimum in the potential energy profile corresponding to the primary form in the ground state. While semi-empirical calculations with CI (AM1/PECI = 8) predict a double well potential, single point density functional theoretic calculations (B3LYP/6-31G**) confirm the absence of a barrier in the ground state for proton transfer. In the first excited singlet state, however, there are two minima corresponding to the primary and tautomeric forms at both ab initio CIS and AM1/PECI = 8 levels, thus accounting for the dual emission in 3HNA. The theoretical methods also account for the observed pH dependence of the spectral characteristics qualitatively correctly. © 2001 Elsevier Science B.V. All rights reserved.

Keywords: 3-Hydroxy-2-naphthoic acid; Excited state intramolecular proton transfer; Hydrogen bonding

1. Introduction

Excited state intramolecular proton transfer (ESIPT) is one of the most important photoexcitation processes occurring in nature. Following the pioneering work of Weller [1,33,34] on salicylic acid (SA) and methyl salicylate (MS), several experimental [2–15,35,36] and theoretical [16–23,37] studies have been devoted to the study of ESIPT processes. Weller interpreted the large Stokes-shifted emission from SA and MS in terms of translocation of a proton from the hydroxyl group to the carboxylic group and also envisaged the formation of a zwitterion in the excited state. Recent [20,22] ab initio electronic structure calculations, however, suggest that ESIPT is not due to zwitterion formation, but due to the motion of the hydrogen atom accompanied by the motion of the other heavy

atoms. Nagaoka and Nagashima [23] suggested that during photo-induced excitation, deformation in benzene ring takes place and that ESIPT occurs in the lowest L_a ($\pi-\pi^*$) state, while L_b ($\pi-\pi^*$) gives normal emission.

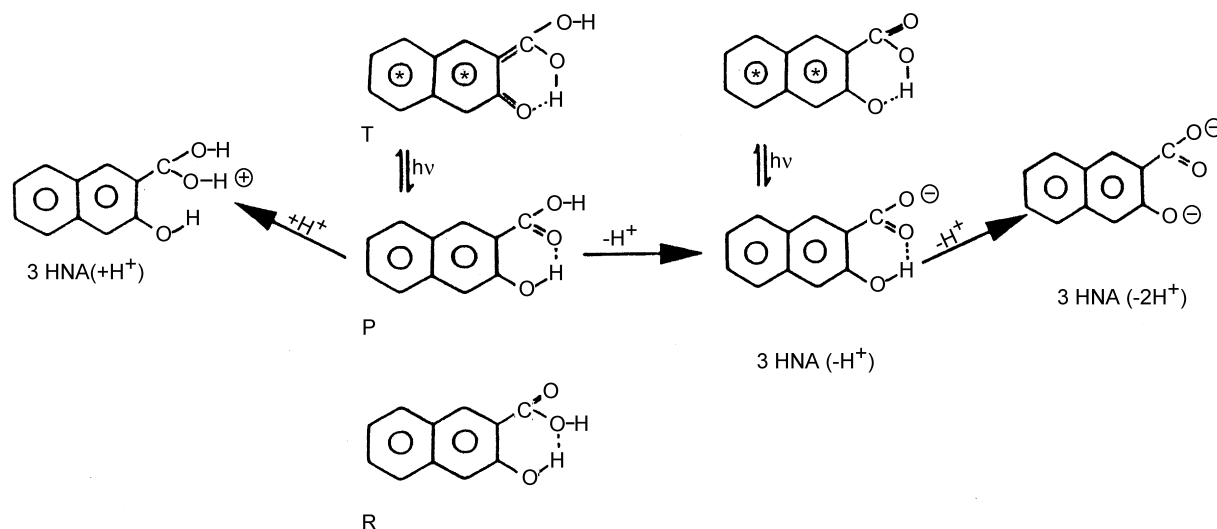
Earlier we had reported on the photophysics of SA in more detail, viz., the effect of dimerization, temperature, hydrogen-bonding solvents and different ionic species on the fluorescence emission from experimental [7–10] as well as theoretical [22] points of view. Subsequently, we have undertaken a detailed investigation of photoexcitation in 3-hydroxy-2-naphthoic acid (3HNA), on which there was only limited information available. Ware et al. [24] had reported the steady state and transient behavior of 3HNA in polar and nonpolar solvents. They found Stokes-shifted emission in acetonitrile, a polar solvent and normal emission in toluene, a nonpolar solvent. However, Stokes-shifted emission was observed when a proton acceptor such as triethylamine (TEA) was added to the nonpolar solvent, indicating ESIPT. Schulman and Kovi [25] have studied the absorption and fluorescence of 3HNA, 2HNA and 1HNA and their dependence on pH. They have attributed the differences in absorption and emission to different species under different conditions. Further they had reported [26,38] that the paths of ionization in ground and excited states

* Corresponding author. Tel.: +91-512-597436/597390;
fax: +91-512-597436.

E-mail address: hirdyesh@yahoo.com (H. Mishra).

¹ Present address: Department of Analytical Chemistry and Applied Spectroscopy, Faculty of Sciences, Vrije Universiteit de Boelelaan 1083, 1081 HV Amsterdam, the Netherlands.

² Honorary Professor, Jawaharlal Nehru Centre for Advanced Scientific Research, Jakkur P.O. Bangalore 560064, India.



Scheme 1. Various emitting species of 3HNA.

were different. They also observed that the excited state photophysics of 3HNA was different from that of SA. The photophysics of methyl 3-hydroxy-2-naphthoate and phenyl 1-hydroxy-2-naphthoate has been reported by Woolfe and Thistlethwaite [3,35]. They have observed that the former gives rise to a large Stokes-shifted emission, while the latter exhibits only a normal fluorescence. This difference has been attributed to the difference in the acid–base properties of the two species. Law and Shoham [27] have also reported on the photophysics of methyl 3-hydroxy-2-naphthoate in nonpolar and polar solvents and found ESIPT to be temperature and solvent dependent. By a comparative study [28] of *t*-butylsalicylic acid and 3HNA, they concluded that the photophysics of the two systems are similar and that ESIPT was necessary for long wavelength emission. Based on their IR studies on 3HNA, Golubev et al. [29] concluded that the presence of *inter* molecular hydrogen bond (in the dimer) affects the strength of the intramolecular hydrogen bond (IMHB). Recently, Catalán et al. [30] have studied the ESIPT in the esters of *o*-hydroxynaphthoic acids and compared the results with those for methyl salicylate. They concluded that the photostability of these compounds are independent of the photophysics of their proton transfer tautomers but it depends upon the non-radiative dynamics of their respective normal tautomers.

Similar to salicylic acid [22], 3HNA can also exist in the form of two ground state conformers P and R as shown in Scheme 1. The former can undergo ESIPT to form the tautomer T, while the latter cannot. Presently, we have carried out a systematic study of steady-state fluorescence emission from 3HNA in different solvents and also in the crystalline phase under different conditions in order to unravel the photophysics of the system. To the best of our knowledge, no electronic structure calculation on substituted naphthoic acid has been reported till this date. Therefore, we have com-

puted the ab initio and semi-empirical potential energy (PE) curves for the ground and ESIPT in 3HNA. The experimental and theoretical results are presented in Sections 2 and 3, respectively. Discussion of the results are given in Section 3 and a summary and conclusion are given in Section 4.

2. Experimental

3HNA (Aldrich) was purified by ethanol–water mixture and recrystallized from ethanol. All the solvents used were of spectroscopic grade (Aldrich) without further purification. Ethanol was made acidic (~ 0.1 M H_2SO_4) and basic (~ 0.1 M KOH) for measurements in low and high pH condition. Absorption spectra were taken with the help of a JASCO V-550 spectrophotometer and fluorescence emission and excitation spectra were recorded using a JASCO FP-777 spectrofluorimeter. The excitation spectra were corrected for detector response and excitation source. However, fluorescence spectra were not corrected. Low temperature measurements were carried out in liquid nitrogen by keeping the sample in a sample holder in a quartz dewar.

3. Results and discussion

3.1. Experimental findings

We have investigated the spectral properties of 3HNA in various solvents/conditions. The spectral data are summarized in Table 1.

3.1.1. Polar solvents

The absorption spectrum of 3HNA under different concentrations in ethanol at room temperature (RT) is

Table 1
Spectral properties of 3HNA in various media

Medium	3HNA (M)	λ_{abs} (nm)	λ_{em} (nm)	Stokes shift (cm^{-1})	Emitting species
EtOH	10^{-3}	360.0	430.0, 515.0	4521, 8360	Neutral and monoanion
EtOH + H^+	10^{-3}	366.0	421.5, 581	4053, 10110	Neutral P, R and T
EtOH + OH^-	10^{-3}	354.0	515.0	8831	Monoanion of T and R
H_2SO_4	10^{-4}	395.6	520.0	6047	Monocation
6 N KOH	10^{-4}	356.0	431.5	4888	Dianion
Water	10^{-4}	354.5	523.5	9106	Monoanion of T and R
Toluene	10^{-5}	355.0	420.0	4359	Neutral P
3MP + IP (glass)	10^{-4}	355.0	400.0 (RT), 400.0, 420.0, 440.0, 525.0 (77 K)	3169 (RT), 9121 (77 K)	Neutral P at RT, dimer at 77 K
Paraffin liquid	Solid	411	530.0 (77 K), 512.0 (RT)	5463, 4799	Dimer
Ether	10^{-4}	360.0	419.0	3267	Weak hydrogen-bonded complex of P
Ether + TEA	10^{-4}	365.0	420.0, 530.0	3968, 8529	Hydrogen-bonded complex of P
Dioxane	10^{-4}	361.0	421.0, 530.0	3948, 8833	Weak hydrogen-bonded complex of P

reproduced in Fig. 1(a). With increase in concentration of 3HNA from 10^{-5} to 10^{-2} M, the absorption maximum (λ_{max}) shifts from 355 to 361 nm. A Stokes-shifted green (G) emission band occurs around 520 nm for 3HNA (10^{-5} M) as shown in Fig. 1(b). With increase in concentration of 3HNA, the intensity of the G band decreases and a violet (V) band develops and grows in intensity at 430 nm as illustrated. Interestingly, the excitation spectrum of the V band is structured, while that of the G band is structureless, as can be seen from Fig. 1(c). Since the $\text{p}K_{\text{a}}$ of 3HNA in water is 4 [15,36], most 3HNA is expected to be in anionic form at low concentrations like 10^{-5} M. Furthermore, the blue shift in absorption maximum with decrease in concentration of 3HNA is akin to that observed when ethanol is made basic (see below). It is also possible that photoexcitation leads to increased emission from the anion in its excited state. Therefore, the G emission reported in Fig. 1(b) can be attributed to the anion and ES IPT therein (Schemes 1 and 2). With increase in concentration, the proportion of the neutral species would increase and one observes a red shift in absorption and also an enhancement in the V band emission, as shown in Fig. 1(a) and (b), respectively. As the spectral behavior of 3HNA is complex in EtOH because of the presence of both the neutral and deprotonated (anionic) species, we have investigated the spectral properties in acidic EtOH, where only neutral species are expected to be present and also in basic EtOH where there will be predominantly the deprotonated species.

In acidic (0.1 M H_2SO_4) ethanol, the absorption spectrum gets slightly red shifted with $\lambda_{\text{max}} = 366$ nm, as shown in Fig. 2(a) for 10^{-3} M 3HNA. The emission spectrum, shown in Fig. 2(b), consists of two bands: one at 421.5 nm (V band) and another very large Stokes-shifted band at 581 nm (R band). The emission spectrum changes with change in excitation wavelength (λ_{ex}) as shown in Fig. 3(a). The intensity of the R band increases with increase in λ_{ex} , while that of the V band decreases. The R band of 3HNA is observed for the first time, although a band at 600 nm was reported earlier by

some workers [3,35] for methyl 3-hydroxy-2-naphthoate. In an earlier work [24] the presence of a base like pyridine was found to be essential for the observation of the Stokes-shifted emission (attributable to ES IPT) in 3HNA. The excitation spectrum of the R band is red shifted when compared to that of the V band, as illustrated in Fig. 3(b). From low temperature measurements, it is found that the red emission band disappears at 77 K and starts reappearing at higher temperatures, as shown in Fig. 4. This suggests proton transfer at higher temperatures.

In basic (0.1 M KOH) ethanol, the absorption maximum is observed at 354 nm (Fig. 2(a)). This is blue shifted, when compared to that in neutral ethanol. Only the G band at 515 nm is observed in the emission spectrum of 3HNA under basic conditions, as shown in Fig. 2(b). In aqueous solution also, only the G band of emission ($\lambda_{\text{max}} = 515$ nm) is observed and the absorption band shows a maximum at 354.5 nm.

3.1.2. Nonpolar solvents

In toluene, 3HNA (10^{-5} M) shows an absorption maximum at 355 nm. It exhibits an emission band (V) that is structured and the corresponding excitation spectrum is also structured. It was not possible to study the spectra at higher concentrations of 3HNA in toluene due to its low solubility. When compared to the acidic solution, the absorption is blue shifted in toluene. In a nonpolar glass mixture (1:1) of 3-methylpentane (3MP) and isopentane (IP), the G band appears at 529 nm at low temperatures as shown in Fig. 5(a). The intensity of this band decreases with increase in temperature and it vanishes completely around 200 K. The excitation spectrum of this band is red shifted as can be seen from Fig. 5(b).

3.1.3. Hydrogen-bonding solvents/reagents

On adding TEA to the solution of 3HNA in toluene, a G band appears at 527 nm. The excitation spectrum of this band is broad and red shifted. Therefore, we have investigated the spectral characteristics of 3HNA in weak hydrogen-bonding

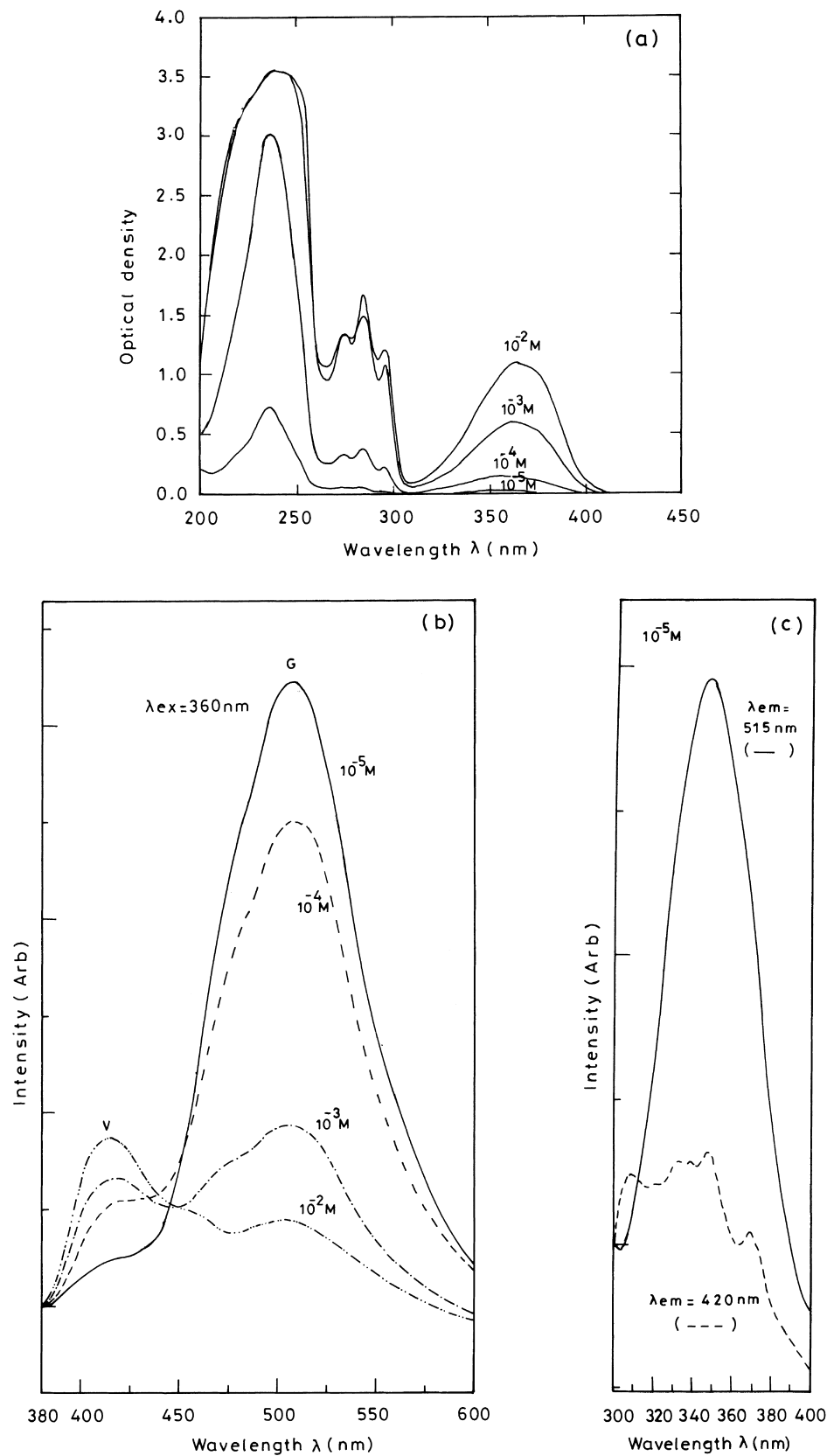


Fig. 1. (a) Absorption and (b) emission spectra of 3HNA at different concentrations in ethanol. (c) Excitation spectra for $\lambda_{em} = 515 \text{ nm}$ (solid line) and $\lambda_{em} = 420 \text{ nm}$ (dashed line) for $10^{-5} M$ 3HNA.

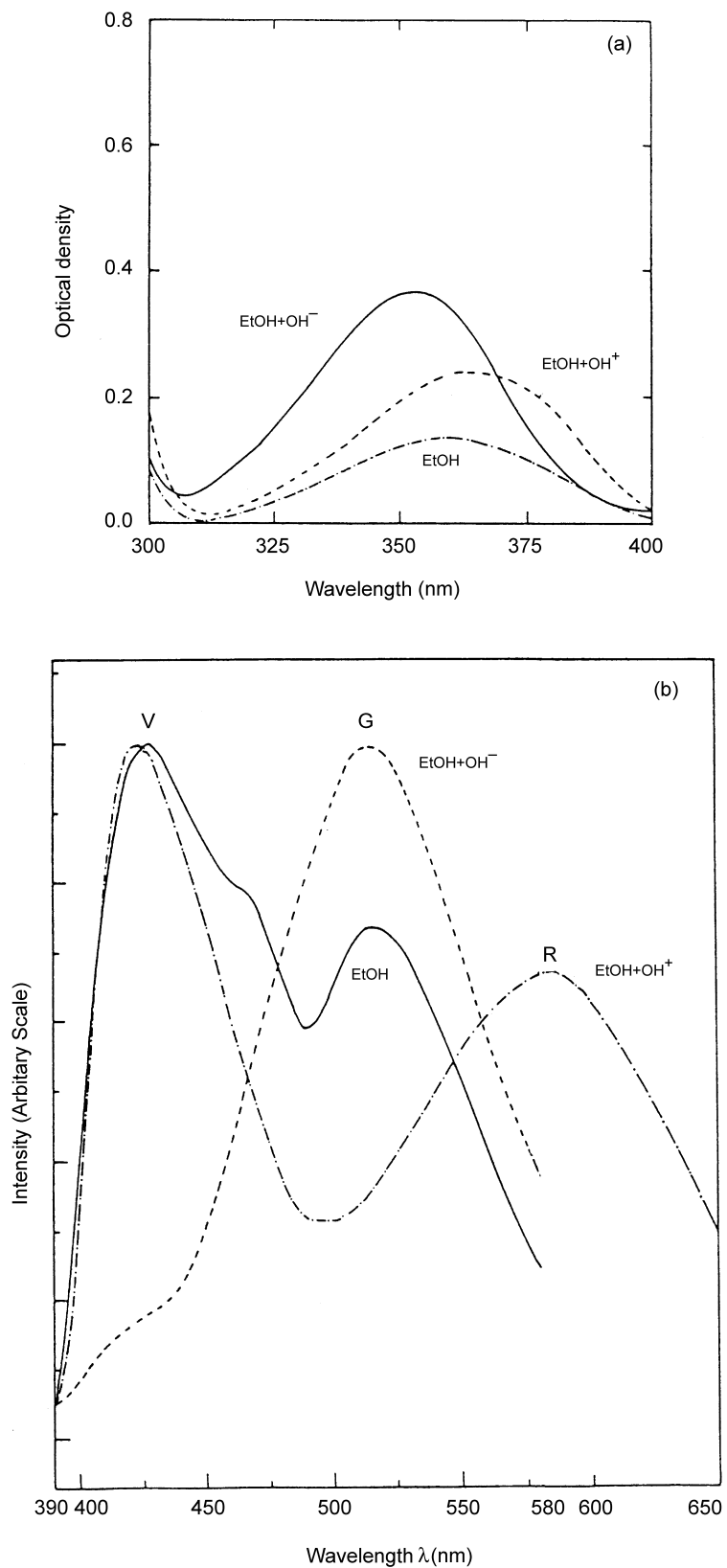


Fig. 2. (a) Absorption spectrum of 10^{-3} M 3HNA in: (i) EtOH; (ii) EtOH + H^+ ; (iii) EtOH + OH^- . (b) Emission spectrum of 3HNA under the same conditions for $\lambda_{ex} = 360$ nm.

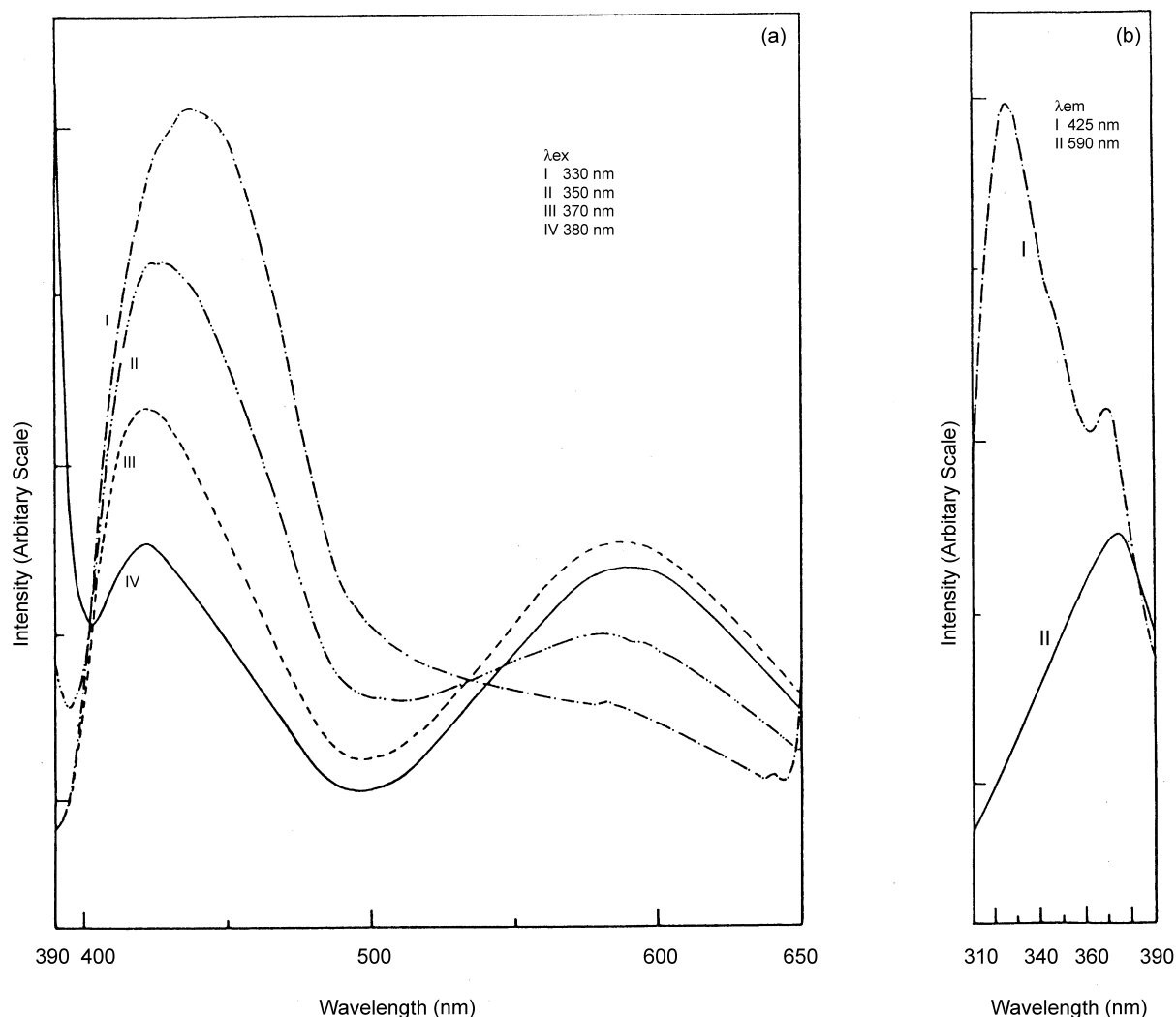


Fig. 3. (a) Emission spectrum of 10^{-3} M 3HNA in acidic ethanol for different λ_{ex} indicated; (b) excitation spectrum corresponding to $\lambda_{\text{em}} = 425$ and 590 nm.

solvents such as diethyl ether and 1,4-dioxane. The absorption maximum occurs at 360 nm for 3HNA in diethyl ether. We observed only the V band emission ($\lambda_{\text{max}} = 419$ nm) and no large Stokes-shifted G band emission (Fig. 6(a)). However, in the presence of a strong hydrogen-bonding substance like TEA, a Stokes-shifted green emission is observed at 526 nm, along with a decrease in intensity of the V band as illustrated in Fig. 6(a). The green emission is strongly dependent on excitation wavelength. Once again the excitation spectrum of the V band is structured while that of the G band is structureless as shown in Fig. 6(b). Similar results have been obtained in 1,4-dioxane solution also.

3.1.4. Low and high pH conditions

In a concentrated H_2SO_4 solution of 3HNA, the absorption maximum occurs at 395.6 nm and the emission shows a maximum at 520 nm. 3HNA is expected to be in its pro-

tonated form (cation) and hence only the normal emission is observed. In 6 N KOH, the absorption maximum occurs at 356 nm and the emission maximum at 431.5 nm. It is expected that 3HNA will exist in its doubly deprotonated form (dianion) under these conditions and only normal emission occurs.

3.2. Theoretical

Our earlier studies [22] have shown that semi-empirical calculations like the AM1/PECI = 8 that include electron pair excitation correlation could predict the absorption λ_{max} , in quantitative accord with the experimental results for SA. But they could not reproduce the essential features of the PE curves, predicted by ab initio calculations like the CASPT2 that include pair excitation correlation. Ab initio calculations at the configuration interaction–single excitation (CIS) level using 6-31G** basis set, e.g., on the other

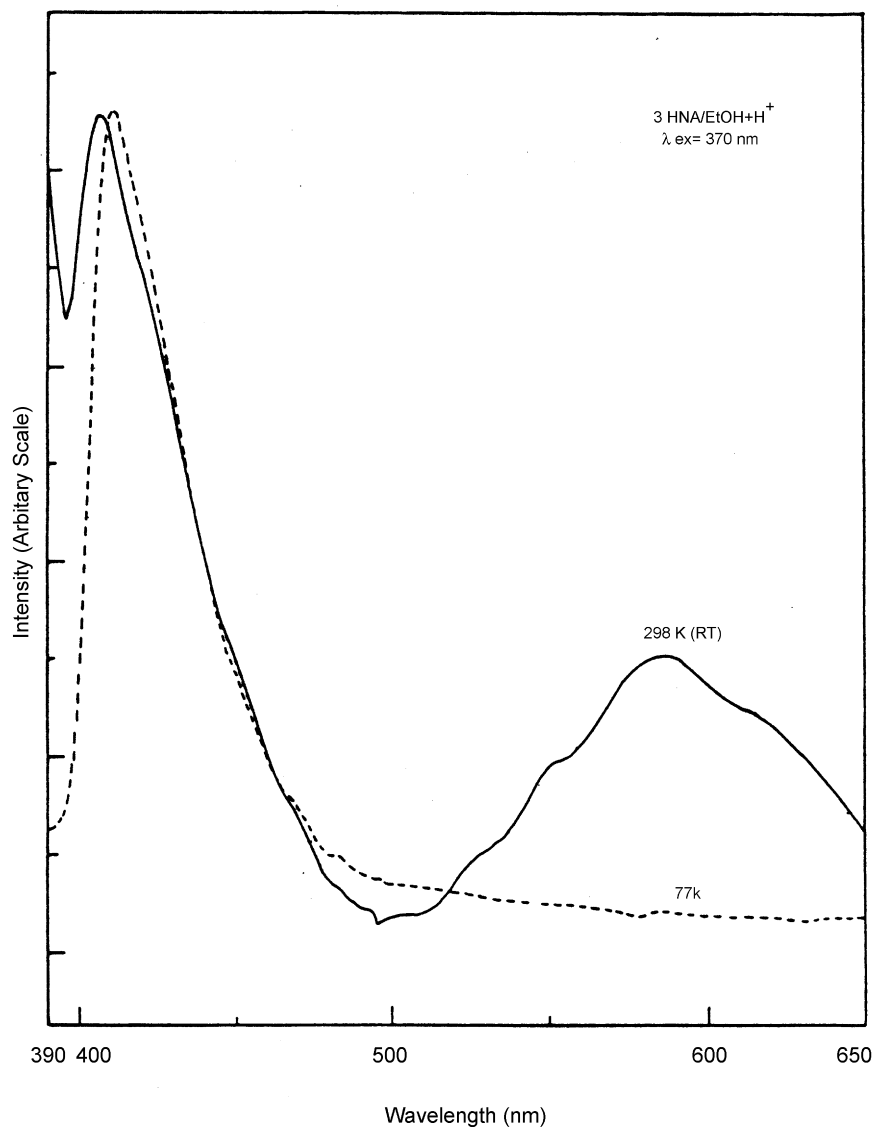


Fig. 4. Emission spectrum of 10^{-3} M 3HNA in acidic ethanol at 298 and 77 K.

hand, could yield reliable PE curves, but were somewhat lacking when it came to predicting λ_{\max} with quantitative accuracy. Nevertheless, such calculations could predict qualitatively correctly the Stokes-shifted emission and red/blue shifts with changing pH conditions. Density functional theoretic (DFT) calculations at the B3LYP/6-31G** level were shown to yield results in quantitative agreement with those from HF/6-31G** calculations for SA. Therefore, we have examined the relative stability of different forms of 3HNA in the ground electronic state, the GSIPT PE curves and also the strength of IMHB, wherever applicable, using AM1/PECI = 8, DFT/B3LYP/6-31G** and HF/6-31G** calculations. Since the above mentioned DFT approach is not immediately applicable to the excited states, we have computed the spectral properties and the ES IPT PE curves for 3HNA at AM1/PECI = 8 and CIS (6-31G**) levels only.

3.2.1. Semi-empirical

The PE profile for the GSIPT for 3HNA obtained from AM1/PECI = 8 calculations reveals two minima, one corresponding to the P form and the other to T. The P form is found to be more stable than the T in the ground electronic state (S_0) by $26.5 \text{ kcal mol}^{-1}$. In the first excited singlet (S_1) state also the P form is more stable than the T, although the difference in energy between the two is only $7.1 \text{ kcal mol}^{-1}$. The strength of the IMHB was found to be $4.6 \text{ kcal mol}^{-1}$ for the P form, $2.8 \text{ kcal mol}^{-1}$ for the R form and $16.0 \text{ kcal mol}^{-1}$ for the T form. There is a large barrier to proton transfer in the ground as well as the first excited state. The computed λ_{\max} for the $S_0 \rightarrow S_1$ transition in 3HNA is 351.4 nm for the P form and 349.4 nm for the R form. For the deprotonated and protonated forms it is 304.2 and 481.4 nm , respectively.

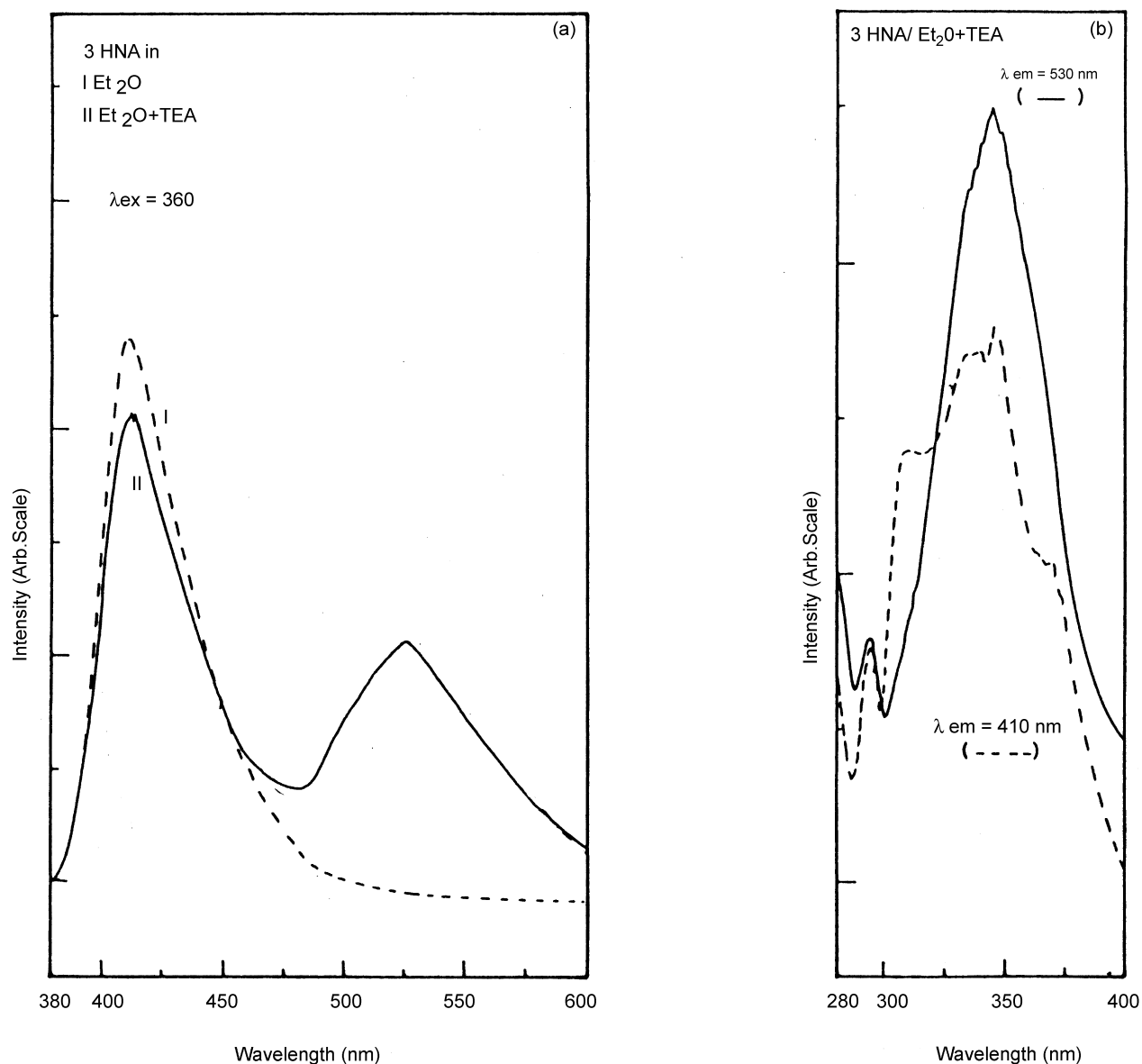


Fig. 5. (a) Emission spectrum of 10^{-4} M 3HNA in a 1:1 mixture of 3MP and IP at different temperatures; (b) excitation spectrum for the same at 77 K for $\lambda_{\text{ex}} = 420$ and 530 nm.

3.2.2. *Ab initio*

Ab initio calculations using the GAUSSIAN 94 suite of programs [31] at the HF (6-31G**) level also show the P form to be the most stable. The T form is higher in energy by 30.3 kcal mol⁻¹. This must be due to the partial loss in aromaticity of the benzene ring arising from proton transfer from P to T, as suggested by Sobolewski and Domcke [19]. The R form is higher in energy than the P only by 3.5 kcal mol⁻¹, and the transformation from P to R involves rotation (τ_1) of the carboxylic acid group, with a barrier of 14.0 kcal mol⁻¹ as shown in Fig. 7.

The strength of the IMHB in the P form of 3HNA was determined to be 9.7 kcal mol⁻¹, by rotating the phenolic OH group out of the hydrogen-bonded configuration and computing the difference in energy between the closed

and open forms. The IMHB was found to be 5.4 and 30.0 kcal mol⁻¹ strong in R and T forms, respectively. DFT/B3LYP/6-31G** calculations yield relative stabilities and the strength of IMHB, in remarkable agreement with the HF/6-31G** results, as shown in Table 2.

The transformation from P to T in the ground electronic state can be thought of as arising from proton transfer from the donating atom O_d to the accepting atom O_a, with concomitant redistribution of electron density in and around the six-membered hydrogen-bonded ring. Alternatively, one could view this as a hydrogen atom transfer. In either case, one needs to identify the “reaction coordinate” and investigate the PE change along the reaction coordinate. Unfortunately, there does not seem to be any simple reaction coordinate definable for the system. It seems reasonable to

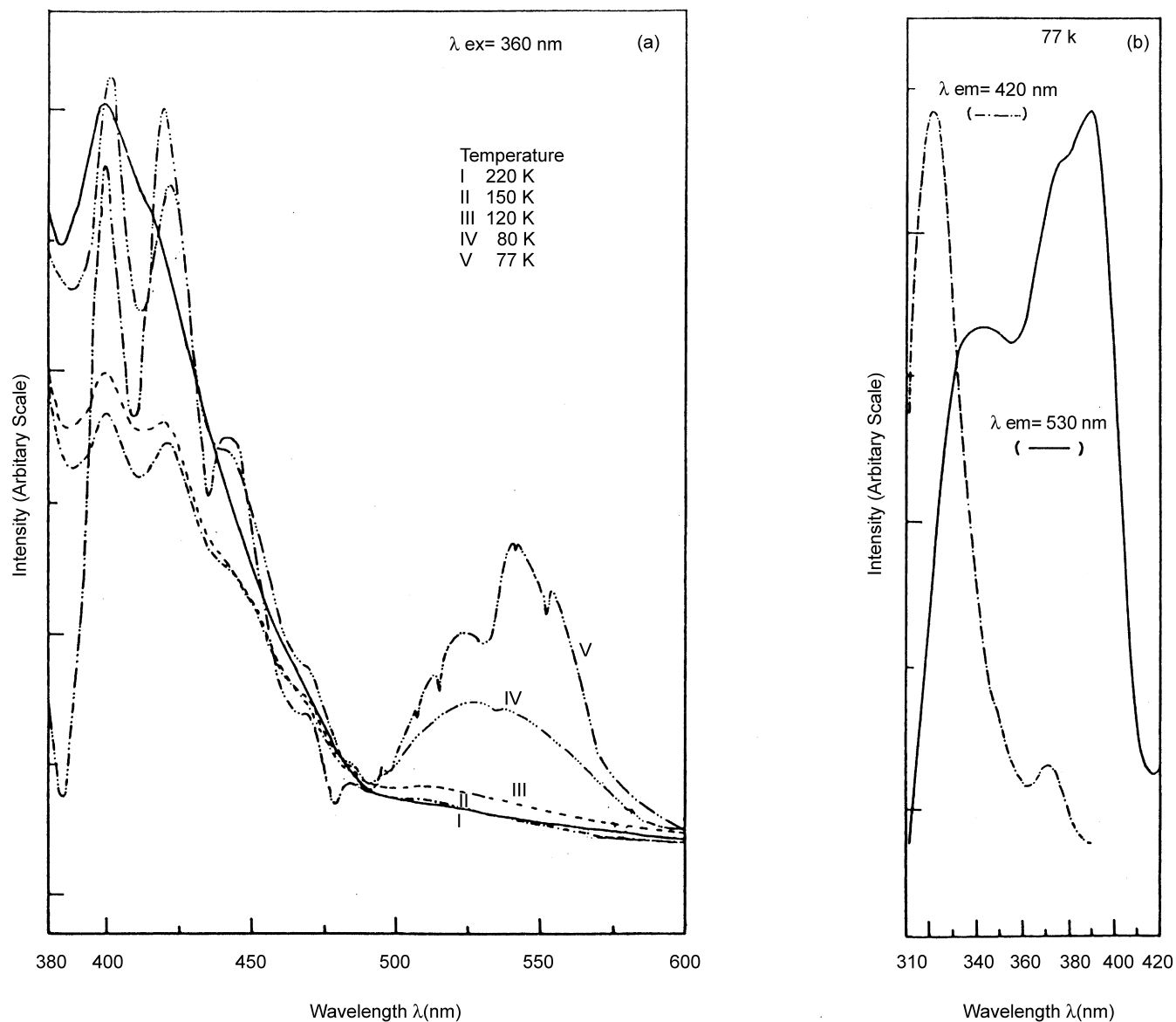


Fig. 6. (a) Emission spectrum of 3HNA in ether and ether + TEA at $\lambda_{\text{ex}} = 360$ nm; (b) excitation spectrum for 3HNA in ether + TEA at $\lambda_{\text{em}} = 410$ and 530 nm.

Table 2

Comparison of relative energies and strengths of IMHBs in different forms of 3HNA and its protonated and deprotonated species in their ground electronic states in kcal/mol units

	Semi-empirical (AM1/PECI = 8)	Ab initio (HF/6-31G**)	DFT (B3LYP/6-31G**//AM1)
<i>Relative stability</i>			
P (enol form)	0.0	0.0	0.0
R (rotamer)	1.6	3.5	3.4
T (keto form)	26.5	30.3	27.6
<i>Strength of IMHB</i>			
P (enol form)	4.6	9.7	10.2
R (rotamer)	2.8	5.4	7.3
T (keto form)	16.0	30.0	25.4
(+H ⁺) (enol form, P)	–	3.6	–
(–H ⁺) (enol form, P)	15.1	25.4	25.3

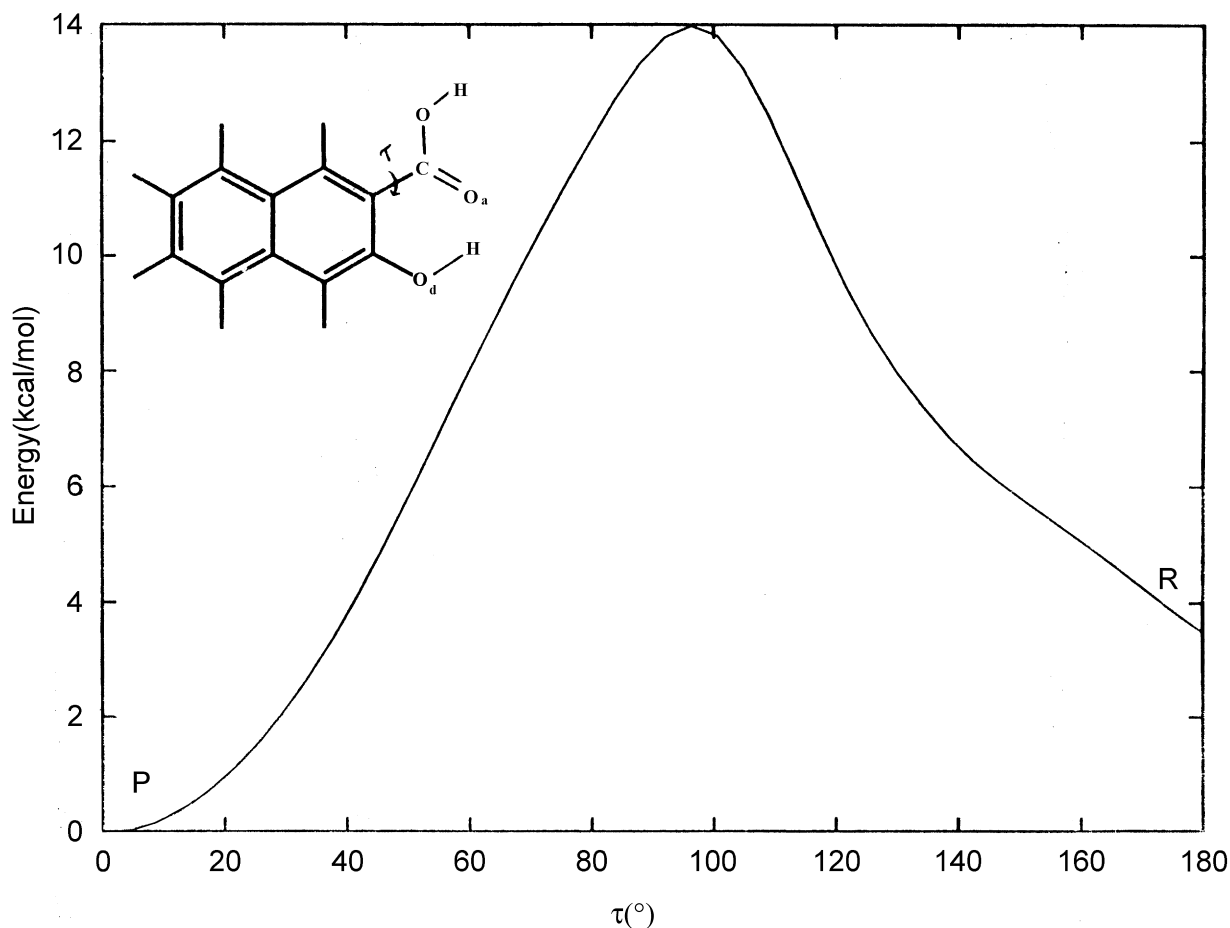


Fig. 7. Energetics of the transformation from the P form of 3HNA to the R. For each value of τ_1 , the geometry has been optimized and energy calculated using HF/6-31G** basis set.

consider stretching of the O_d-H bond distance r_{O_d-H} and contracting of the $H-O_a$ bond distance r_{O_a-H} as constituting the reaction coordinate. Some authors have considered the $O_d \cdots O_a$ distance as fixed and varied r_{O_d-H} . This may not be appropriate as it puts avoidable constraints on the system. We have therefore chosen to vary r_{O_d-H} and optimize the rest of the structural parameters for each choice of r_{O_d-H} . This is sometimes referred to as the “distinguished-coordinate” approach in the literature [20]. The resulting PE profile for GSIPT, shown in Fig. 8, reveals that the P form is the most stable (as stated above). And there is no “well” for the T form, implying that GSIPT is unlikely.

The PE profiles obtained from CIS calculations for the first three excited $^1A'$ states of 3HNA are included in Fig. 8. The absorption maximum (λ_{max}) for the P form works out to be 253 nm, when compared to the experimental value of 360 nm in ethanol. This discrepancy is not surprising because we have only included single excitations in the ab initio calculation. We hope that the qualitative features of the PE curves for the different electronic states obtained are still reliable.

It is clear from Fig. 8 that the P form is the most stable in the lowest excited singlet (S_1) state also. Although there is

a $9.1 \text{ kcal mol}^{-1}$ barrier to proton transfer in S_1 , it must be pointed out that the PE curve is relatively shallow, indicating that emission from the excited state can take place over a range of geometries. The variation of oscillator strength (f) with r_{O_d-H} is shown in Fig. 9 for the S_0-S_1 transition. Interestingly, f for S_0-S_2 is twice that for S_0-S_1 and f for S_0-S_3 is an order of magnitude larger. This is in keeping with the intensities of the three different absorption bands shown in Fig. 1(a). CIS calculations for the R form predict the λ_{max} for absorption to be 250 nm. Analysis of the MOs involved in the transition suggests it to be $\pi-\pi^*$, same as for P. Since there is no likelihood of proton transfer in R, the PE curves have a single minimum in the ground and first excited singlet states (not shown).

Our earlier calculations [22] for salicylic acid had shown that the computed λ_{max} for gaseous condition (dielectric constant $\epsilon = 1.0$) remained essentially unaltered, when ϵ was changed, within the self-consistent reaction field method, based on the Onsager reaction field model [32]. Therefore we have not computed λ_{max} for different values of ϵ . With the addition of a mineral acid, 3HNA gets protonated and with the addition of a base, it gets deprotonated, as illustrated in Scheme 1. The PE profiles for intramolecular proton trans-

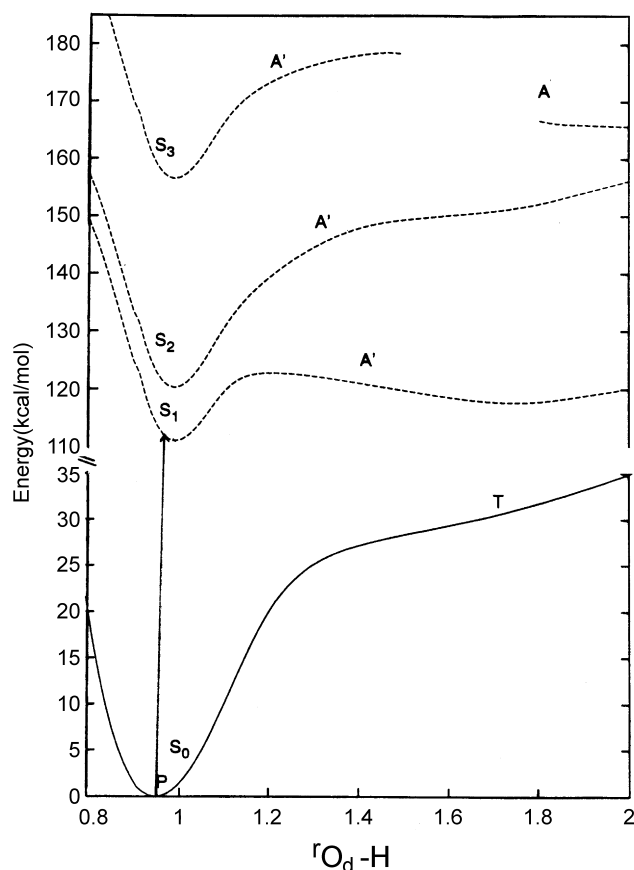


Fig. 8. PE profile for intramolecular proton transfer in the ground and excited states of 3HNA.

fer in the protonated species, shown in Fig. 10 reveal a single well for the ground state and also for the lowest excited $^1A'$ (S_1) state. The lack of proton transfer is reinforced by a weak IMHB ($\sim 3.64 \text{ kcal mol}^{-1}$) in the protonated species. The λ_{max} computed for the $S_0 \rightarrow S_1$ transition in the protonated species is 330 nm, when compared to 395 nm observed experimentally. Qualitatively, this means that the ab initio calculations are able to predict the observed red shift in λ_{max} due to protonation correctly.

As mentioned above, 3HNA gets deprotonated with increase in pH. But this involves a stronger IMHB ($25.4 \text{ kcal mol}^{-1}$). The PE profiles for the deprotonated species shown in Fig. 11 reveal that both P and T forms are stable, giving rise to a double well potential, in the ground state. In the first excited $^1A'$ (S_1), however, the tautomeric form is more stable (by $18.0 \text{ kcal mol}^{-1}$) than the primary. Thus, interestingly, the asymmetric double well potentials proposed by Weller seem to be appropriate for the deprotonated 3HNA. The λ_{max} computed for the deprotonated species is 241 nm, when compared to 354 nm observed experimentally. Thus ab initio theory predicts correctly a blue shift with deprotonation. At very high pH, 3HNA loses both the acidic protons and the resulting dianion has a $\lambda_{\text{max}} = 303 \text{ nm}$, compared to 356 nm observed experimentally.

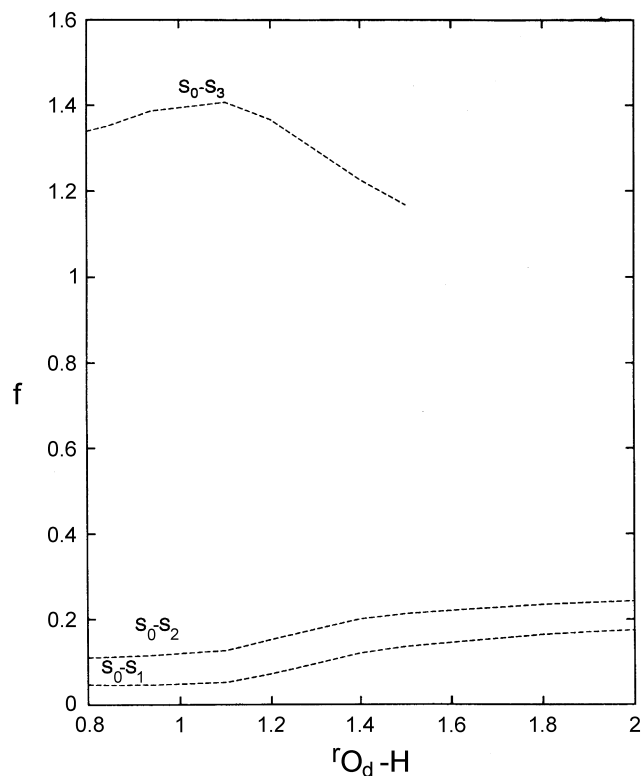


Fig. 9. Oscillator strengths (f) for the S_0-S_1 , S_0-S_2 and S_0-S_3 transitions of 3HNA as a function of $r_{O_d}-H$.

The neutral 3HNA molecule is expected to be present largely in the P form and to a much less extent in R, as the former is lower in energy by $3.5 \text{ kcal mol}^{-1}$. The V band emission can be identified as arising from the R form as it is blue shifted and the excitation spectrum is structured. There is no ES IPT in the R form as it becomes evident from the single well in the PE profile for the ground as well as the excited state. In acidic ethanol, 3HNA is expected to be present predominantly as the neutral P form. The large Stokes-shifted ($10,110 \text{ cm}^{-1}$) emission presumably arises from the tautomer resulting from ES IPT in the P form. Such a large Stokes-shifted emission from the excited state of the P form is also predicted by theoretical calculations (see Table 3), which indicate a double well-potential profile for the excited state. In slightly basic ethanol, the Stokes-shifted

Table 3
Absorption maxima (λ_{max}) and Stokes shifts for 3HNA and its protonated and deprotonated species, as obtained from theory and experiment

Species	λ_{max} (nm)/Stokes shift (cm^{-1})		
	AM1/PECI = 8	CIS/6-31G**	Experiment
P (enol form)	351.4/6783	253/9856	360.0/10,110
R (keto form)	349.4	250	355
($-H^+$) (enol form)	304.2/8977	242/8248	354/8831
($+H^+$) (enol form)	481.4/4549	330/5571	396/6047
($-2H^+$)	–	303	356

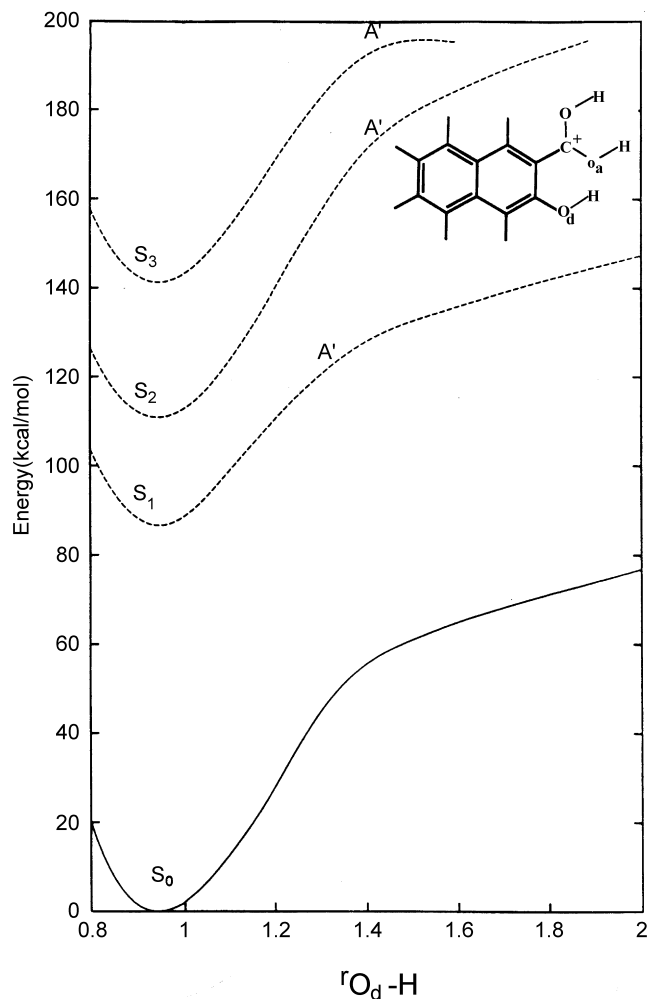


Fig. 10. PE profile for intramolecular proton transfer in the ground and excited states of 3HNA in its protonated form.

emission at 515 nm, presumably comes from the anion of 3HNA. Strength of the IMHB increases in going from the neutral to the anionic species, in ground as well as the first excited state. The T form is more stable than the P in the excited state. Hence only the band arising from ESIPT is observed. In an aqueous solution also, 3HNA exists largely in the deprotonated form and it gives only the G band.

Under very high pH (6N KOH) conditions, the anion gets further deprotonated, resulting in the dianion. The PE profiles indicate a single well for both ground and excited states, thus predicting normal emission.

In a concentrated H_2SO_4 solution, 3HNA would exist in its protonated form. Theoretical studies predict a single well PE curve for the ground as well as the excited state. Therefore it is understandable that only normal emission takes place at low pH. In an acidic ethanol solution of 3HNA, the red band emission disappears at 77 K, presumably due to decreased ESIPT. While in basic ethanol medium, the intensity of the G band increases with decrease in temperature due to reduction in non-radiative processes. In nonpolar sol-

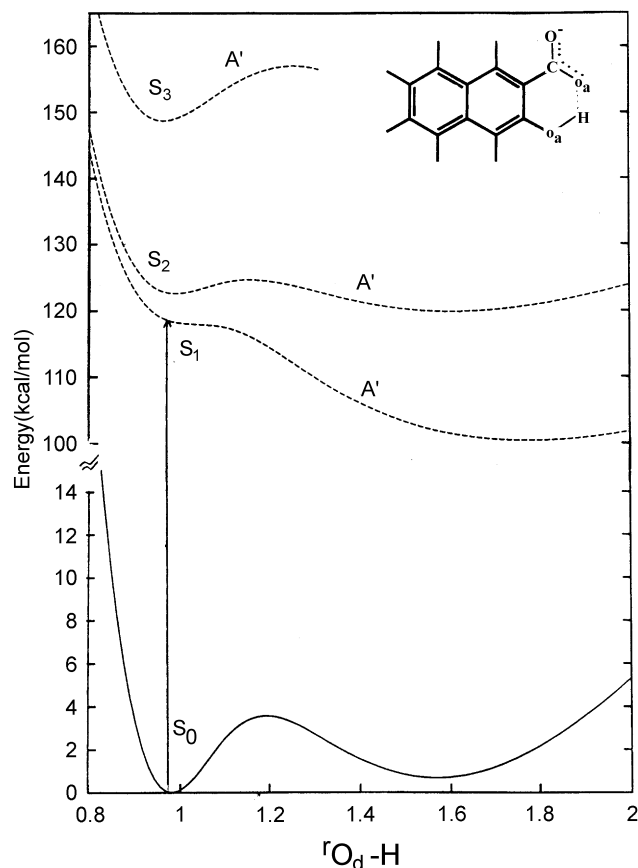
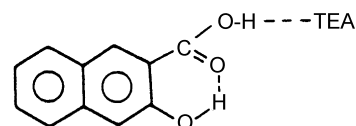


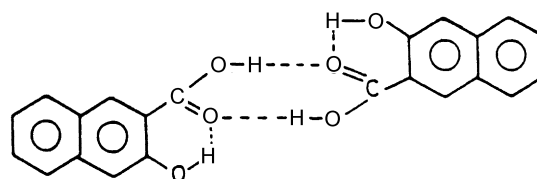
Fig. 11. PE profile for intramolecular proton transfer in the ground and excited states of 3HNA in its deprotonated form.

vents, large Stokes-shifted R band could not be observed. The appearance of the G band in the presence of TEA must be due to the formation of strong *intermolecular* hydrogen bond with the carboxylic group proton, which increases the strength of the IMHB thus facilitating ESIPT, as shown in Scheme 2.

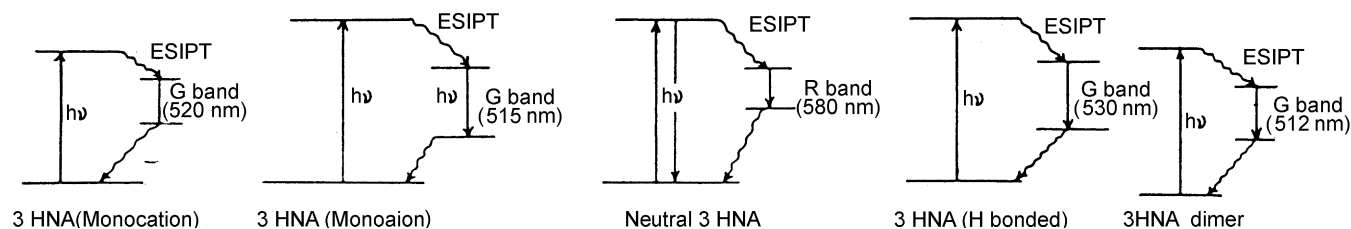
The appearance of the G band at low temperatures in nonpolar solvents without adding TEA can be attributed to the formation of the cyclic dimer (see Scheme 3), which



Scheme 2. Hydrogen-bonded complex of 3HNA with TEA.



Scheme 3. 3HNA dimer of P form.



Scheme 4.

undergoes ESIPT. The various emissions described above are represented schematically in Scheme 4.

4. Summary and conclusion

Experiments show that 3HNA, on photoexcitation exhibits dual emission corresponding to normal and large Stokes-shifted fluorescence. The latter is attributed to emission following ESIPT. The absorption and emission characteristics are shown to be sensitive to the concentration of 3HNA, the choice of solvent, pH, temperature and excitation wavelength. 3HNA forms different species in different media. A large Stokes-shifted emission from 3HNA in acidic ethanol is being reported for the first time. In basic ethanol, the anion is formed and it undergoes ESIPT, but the Stokes shift is much smaller.

Semi-empirical calculations (AM1/PECI = 8) predict the absorption λ_{\max} in accord with experiment for 3HNA, and its protonated and deprotonated species. Ab initio calculations at the CIS/6-31G** level do not yield λ_{\max} with quantitative accuracy, but predict the Stokes shifts in agreement with the experimental results. In addition, it is to be pointed out that the ground electronic state PE curves for 3HNA and 3HNA(+H⁺) yield a single minimum corresponding to the P form. The first excited electronic state PE curve does show a double minimum for 3HNA, but a single minimum for the protonated species. In the case of the deprotonated species, the ground state PE curve has a double minimum, while the first excited singlet state curve has a single minimum corresponding to the tautomeric form, pointing out that ESIPT is more facile in the anion than in the neutral or protonated forms of 3HNA. The red and blue shifts in emission predicted by theory are in qualitative accord with the experimental findings.

Acknowledgements

The authors are thankful to DST (under National LASER Programme) and UGC (DSA) for financial assistance. We are grateful to Dr. D.D. Pant for his valuable discussions. HM, SM and MP are grateful to CSIR, New Delhi for their fellowships.

References

- [1] A. Weller, *Naturwissenschaften* 42 (1955) 175.
- [2] W. Klopffer, *Adv. Photochem.* 10 (1977) 311.
- [3] G.J. Woolfe, P.J. Thistlethwaite, *J. Am. Chem. Soc.* 102 (1980) 6917.
- [4] K.K. Smith, K.J. Kaufmann, *J. Phys. Chem.* 85 (1981) 2895.
- [5] F. Torobio, J. Catalán, F. Amat, A.U. Acuna, *J. Phys. Chem.* 87 (1983) 817.
- [6] J.L. Herek, S. Pedersen, L. Bañares, A.H. Zewail, *J. Chem. Phys.* 97 (1992) 9046.
- [7] H.C. Joshi, H.B. Tripathi, T.C. Pant, D.D. Pant, *Chem. Phys. Lett.* 173 (1990) 83.
- [8] D.D. Pant, H.C. Joshi, P.B. Bisht, H.B. Tripathi, *Chem. Phys.* 185 (1994) 137.
- [9] P.B. Bisht, H.B. Tripathi, D.D. Pant, *J. Photochem. Photobiol. A* 90 (1995) 103.
- [10] H.C. Joshi, H. Mishra, H.B. Tripathi, *J. Photochem. Photobiol. A* 105 (1997) 15.
- [11] P.B. Bisht, H. Petek, K. Yoshihara, U. Nagashima, *J. Chem. Phys.* 103 (1995) 5290.
- [12] P.B. Bisht, M. Okamoto, S. Hirayama, *J. Phys. Chem. B* 101 (1997) 8850.
- [13] F. Lahmani, A. Zehnacker-Rentien, *J. Phys. Chem. A* 101 (1997) 6141.
- [14] B. Humbert, M. Alnot, F. Quilés, *Spectrochim. Acta A* 54 (1998) 465.
- [15] G.S. Denisov, N.S. Golubev, V.M. Schreiber, Sh.S. Shajakhmedov, A.V. Shurukhina, *J. Mol. Struct.* 381 (1996) 73.
- [16] J. Catalán, J.I. Fernandez-Alonso, *Chem. Phys. Lett.* 18 (1973) 37.
- [17] J. Catalán, J. Palomar, J.L.G. de Paz, *J. Phys. Chem.* 101 (1997) 7914.
- [18] M.V. Vener, S. Scheiner, *J. Phys. Chem.* 99 (1995) 642.
- [19] A.L. Sobolewski, W. Domcke, *Chem. Phys.* 184 (1994) 115.
- [20] A.L. Sobolewski, W. Domcke, *Chem. Phys.* 232 (1998) 257.
- [21] S. Mitra, R. Das, S.P. Bhattacharyya, S. Mukherjee, *J. Phys. Chem.* 101 (1997) 293.
- [22] S. Maheshwari, A. Chowdhury, N. Sathyamurthy, H. Mishra, H.B. Tripathi, M. Panda, J. Chandrasekhar, *J. Phys. Chem.* 103 (1999) 6257.
- [23] S. Nagaoka, U. Nagashima, *Chem. Phys.* 136 (1989) 153.
- [24] W.R. Ware, P.R. Shukla, P.J. Sullivan, R.V. Bremplis, *J. Chem. Phys.* 55 (1971) 4048.
- [25] S.G. Schulman, P.J. Kovi, *Anal. Chim. Acta* 67 (1973) 259.
- [26] P.J. Kovi, S.G. Schulman, *Anal. Chem.* 45 (1973) 989.
- [27] K.Y. Law, J. Shoham, *J. Phys. Chem.* 98 (1994) 3114.
- [28] K.Y. Law, J. Shoham, *J. Phys. Chem.* 99 (1995) 12103.
- [29] N.S. Golubev, G.S. Denisov, L.A. Kuzina, S.N. Smirnov, *J. Gen. Chem. Russia* 64 (1994) 1162.
- [30] J. Catalán, J.C. del Valle, J. Palomar, C. Díaz, J.L.G. de Paz, *J. Phys. Chem. A* 103 (1999) 10921.
- [31] Gaussian 94, Revision C.2, M.J. Frisch, G.W. Trucks, H.B. Schlegel, P.M.W. Gill, B.G. Johnson, M.A. Robb, J.R. Cheeseman, T. Keith, G.A. Petersson, J.A. Montgomery, K. Raghavachari, M.A. Al-Laham,

- V.G. Zakrzewski, J.V. Ortiz, J.B. Foresman, J. Cioslowski, B.B. Stefanov, A. Nanayakkara, M. Challacombe, C.Y. Peng, P.Y. Ayala, W. Chen, M.W. Wong, J.L. Andres, E.S. Replogle, R. Gomperts, R.L. Martin, D.J. Fox, J.S. Binkley, D.J. Defrees, J. Baker, J.P. Stewart, M. Head-Gordon, C. Gonzalez, J.A. Pople, Gaussian Inc., Pittsburgh, PA, 1995.
- [32] L. Onsager, *J. Am. Chem. Soc.* 58 (1938) 1486.
- [33] A. Weller, *Z. Electrochem.* 60 (1956) 1144.
- [34] A. Weller, *Prog. React. Kinet.* 1 (1961) 187.
- [35] G.J. Woolfe, P.J. Thistlethwaite, *J. Am. Chem. Soc.* 103 (1981) 3849.
- [36] G.S. Denisov, N.S. Golubev, V.M. Schreiber, Sh.S. Shajakhmedov, A.V. Shurukhina, *J. Mol. Struct.* 436 (1997) 153.
- [37] J. Catalán, J.I. Fernandez-Alonso, *J. Mol. Struct.* 27 (1975) 59.
- [38] P.J. Kovi, C.L. Miller, S.G. Schulman, *Anal. Chim. Acta* 61 (1972) 7.